Adaptively Determination of Model Order of SVD-based Harmonics and Interharmonics Estimation

Jian Song[1, 3], Liang Zhu[2], Alessandro Mingotti[3], Lorenzo Peretto[3], He Wen[1]
[1]College of Electrical and Information Engineering - Hunan University, Changsha, P.R. China
Email: songjian1705@126.com, he_wen82@126.com
[2]Power Supply Service Management Center of State Grid Jiangxi Electric Power Co., Ltd., Nanchang, P.R. China
Email: fastspeed008@126.com
[3]Department of Electrical, Electronic and Information Engineering - University of Bologna, Bologna, Italy
Email: alessandro.mingotti2@unibo.it, lorenzo.peretto@unibo.it

***Abstract*—The singular value decomposition (SVD) is one of the most popular methods in harmonics and interharmonics estimation. However, its accuracy strongly depends on the correctness of the selected model order. To this purpose, this work aims at contributing to the correct estimation of the model order. This is achieved by exploiting the energy of the singular values (SVs). Firstly, the relationship between one frequency component and its corresponding SVs is theoretically investigated. Secondly, a new indicator is proposed for determining the model order, which denotes the energy of the *k*-th pair of consecutive SVs. Thirdly, an adaptive threshold is defined for separating signal components from noise. This way, the number of components can be obtained for unknown noise levels. Finally, the effectiveness and robustness of the proposed method has been validated by simulations. They have been run implementing typical signals designed according to the harmonics and interharmonics measurements standard, the IEC standard 61000-4-7.**

Keywords—Model order determination, singular value decomposition, harmonics estimation, interharmonics estimation

I. Introduction

The proliferation of power electronics based non-linear loads is worsening the power quality (PQ) of the power system. In particular, the presence of harmonics and interharmonics components affects it the most. [1-4]. Therefore, their accurate estimation is essential for the safe and stable operation of the grid. At present, the estimation methods can be divided into two main categories: Discrete Fourier Transform (DFT) based methods and Singular Value Decomposition (SVD) based methods (i.e., the modern spectral estimation method) [5-10].

Due to its high-resolution feature in the frequency domain, the SVD-based methods have received considerable scholarly attention. This is particularly true within the field of the analysis of harmonics and interharmonics [11]. The SVD-based method includes the Prony method [12], the Matrix Pencil [13-15], and the estimation of signal parameters via rotational invariance techniques (ESPRIT) [5, 16-18]. Generally, accurate estimates of harmonics and interharmonics can be achieved by all these methods under the premise that a proper model order (i.e., the number of the signal components) is offered. An incorrect model order, whether it is higher or lower than the correct one, will dramatically deteriorate the performance of these methods. Consequently, a robust model order estimation technique, for harmonics and interharmonics, is crucial in the SVD-based approaches.

To solve such a problem, different methods based on SVs have been developed to estimate an exact value of the model order. In [11, 13, 14], methods for determining the model order, which relied on the ratio of SVs to the max one, are presented. The ratio was compared with fixed thresholds that were selected experimentally under specific noise level and observation window lengths. However, these heuristically determined thresholds cannot adapt to conditions in which noise can vary over time. In [16] and [19], a method based on selected relative difference index of SVs is introduced to estimate the model order in the presence of varying noise levels and data window lengths. Nevertheless, the method needs to determine the sensitivity factor for different levels of noise. An improved version of [19], called modified exact model order (MEMO), is proposed in [5]. This method not only does not require any threshold parameters but also returns more reliable estimates, regardless of the length of the data window. However, if small relative difference exists between the SVs components and noise, the MEMO method usually fails. This is because significant relative difference may not exist between the signal and the 'noise' components under low signal-to-noise ratio (SNR) scenarios.

Although raw SVs are used to estimate the model order of a signal containing harmonics and interharmonics, literature lacks documentation about the relationship between one frequency component and its corresponding SVs. Therefore, this work starts exactly from this task, with the higher aim of distinguishing the weak harmonics or interharmonics from noise independently. Then, a new indicator is proposed for determining the model order, which denotes the energy of the *k*-th pair of consecutive SVs. Finally, an adaptive threshold is introduced for separating the signal components from unknown noise levels. This way it is possible to determine the number of components at unknown noise levels. The efficiency and applicability of the method have been validated, by simulations, with a variety of typical signals defined according to IEC standard 61000-4-7.

II. Proposed Model Order Determination Method

A. Signal Model of Multifrequency Power Signal

In the following, let us consider the sampled distorted power supply signals of length N (n = 0, 1, ..., N-1):

$$y(n) = y(t)\big|_{t=nT_s} = \sum_{k=1}^{K} A_k \cos\left(2\pi f_k n T_s + \phi_k\right) + w(n), \quad (1)$$

where K is the model order (the number components), f_k, A_k, and ϕ_k are, respectively, the frequency, amplitude, and phase of the k-th component. For k = 1, f_1, A_1, and ϕ_1 are the parameters of fundamental component. $T_s = 1/f_s$ is the sampling interval, and f_s is the sampling rate, and $w(n)$ represents the white Gaussian noise with zero mean.

B. The Relationship Between the Frequency Component and Its Corresponding SVs

In general, two steps are required for determining the model order of an SVD-based method for harmonics and interharmonics estimation. The first step is the generation of the Hankel matrix $\boldsymbol{H}$ by using N data samples of the measured signal $y(n)$, as:

$$\boldsymbol{H}=\begin{bmatrix} y(1) & y(2) & \cdots & y(L) \\ y(2) & y(3) & \cdots & y(L+1) \\ \vdots & \vdots & \cdots & \vdots \\ y(L) & y(L+1) & \cdots & y(N) \end{bmatrix}, \tag{2}$$

where $L = (N + 1)/2$. For simplicity, N here is specified as odd to obtain a square Hankel matrix $\boldsymbol{H}$, and L is specified as even.

The second step is the application of SVD on $\boldsymbol{H}$ as:

$$\boldsymbol{H}=\boldsymbol{U}\boldsymbol{S}\boldsymbol{V}^{\mathrm{H}}, \tag{3}$$

where $(\,)^{\mathrm{H}}$ represents the Hermitian transpose operator, $\boldsymbol{U}=[\boldsymbol{u}_{11}, \boldsymbol{u}_{12},..., \boldsymbol{u}_{G1}, \boldsymbol{u}_{G2}]$ and $\boldsymbol{V}=[\boldsymbol{v}_{11}, \boldsymbol{v}_{12},..., \boldsymbol{v}_{G1}, \boldsymbol{v}_{G2}]^{\mathrm{T}}$ are $L\times L$ unitary matrixes. $\boldsymbol{S}$ is a $L\times L$ diagonal matrix which contains SVs of $\boldsymbol{H}$ and can be expressed as:

$$\boldsymbol{S}=\mathrm{diag}\left[\sigma_{11},\sigma_{12},\cdots,\sigma_{k1},\sigma_{k2},\cdots,\sigma_{G1},\sigma_{G2}\right], \tag{4}$$

where $G = L/2$, $\sigma_{11} \geq \sigma_{12} \geq ... \geq \sigma_{k1} \geq \sigma_{k2} \geq ... \geq \sigma_{G1} \geq \sigma_{G2}$.

It is known that two consecutive SVs correspond to a frequency component of a distorted signal [5]. So, σ_{k1} and σ_{k2} are considered as a pair of SVs taken from the k-th component.

1) Energy defined by SVs and Frobenious norm

Substituting (1) into (2), $\boldsymbol{H}$ can be indicated as the superposition of a series of sub-matrix $\boldsymbol{H}_k$ as:

$$\boldsymbol{H}=\boldsymbol{H}_1+\ldots+\boldsymbol{H}_k+\ldots+\boldsymbol{H}_K+\boldsymbol{H}_w, \tag{5}$$

where $\boldsymbol{H}_w$ represents the Hankel matrix including noise interference, and $\boldsymbol{H}_k$ refer to the Hankel matrix obtained with the k-th frequency component as:

$$\boldsymbol{H}_k=\begin{bmatrix} y_k(1) & y_k(2) & \cdots & y_k(L) \\ y_k(2) & y_k(3) & \cdots & y_k(L+1) \\ \vdots & \vdots & \cdots & \vdots \\ y_k(L) & y_k(L+1) & \cdots & y_k(N) \end{bmatrix}, \tag{6}$$

where $y_k(n)=A_k\cos\left(2\pi f_k n T_s+\phi_k\right)$.

According to the definition of the Frobenious norm (F-norm) of $\boldsymbol{H}$ [20], one have:

$$\left(\|\boldsymbol{H}\|_F\right)^2=\sum_{r=1}^{L}\sum_{c=1}^{L}\left(\boldsymbol{H}(r,c)\right)^2=\sum_{k=1}^{G}(\sigma_{k1}^2+\sigma_{k2}^2), \tag{7}$$

where $\|\ \|_F$ represents the F-norm operator, r and c are the index of row and column, respectively. To better understand the relationship between the k-th component and σ_{k1} and σ_{k2}, it is introduced the notation $\hat{\boldsymbol{E}}_k=\sigma_{k1}^2+\sigma_{k2}^2$. It is an indicator, for determining the model order, which denotes the energy of the k-th pair of consecutive SVs. In addition, to denote the energy of the Hankel matrix $\boldsymbol{H}$ and the k-th component the notations $\boldsymbol{E}=\left(\|\boldsymbol{H}\|_F\right)^2$ and $\boldsymbol{E}_k$ are introduced, respectively.

2) Energy $\boldsymbol{E}$ expressed by the parameters of the components

Firstly, the energy of a single element $\boldsymbol{H}(r,c)$ in $\boldsymbol{H}$ can be expressed as:

$$\begin{aligned}\boldsymbol{E}_{r,c}&=\left(\boldsymbol{H}(r,c)\right)^2\\&=\left(\sum_{k=1}^{K}\boldsymbol{H}_k(r,c)\right)^2\\&=\sum_{k=1}^{K}\left(y_k(n)\right)^2+\sum_{i=1}^{K}\sum_{\substack{j=1\\ j\neq i}}^{K}\left(y_i(n)y_j(n)\right)\end{aligned}, \tag{8}$$

where r = 1, 2, ..., L, c = 1, 2, …, L, and $n = r + c$ - 1.

Secondly, the energy of the r-th row in the $\boldsymbol{H}$ can be obtained by summing the energies of all elements in this row as:

$$\begin{aligned}\bar{\boldsymbol{E}}_r&=\sum_{c=1}^{L}\left(\boldsymbol{E}_{r,c}\right)\\&=\sum_{n=r}^{L+r-1}\left(\sum_{k=1}^{K}\left(y_k(n)\right)^2+\sum_{i=1}^{K}\sum_{\substack{j=1\\ j\neq i}}^{K}\left(y_i(n)y_j(n)\right)\right)=\overset{\Theta}{\boldsymbol{E}}_r+\overset{\Delta}{\boldsymbol{E}}_r\end{aligned}, \tag{9}$$

where

$$\overset{\Theta}{\boldsymbol{E}}_r=\sum_{k=1}^{K}\left(\frac{A_k^2}{2}\left(L+\Re_k\cos\left(2\pi f_k T_s(L+2r-1)+2\phi_k\right)\right)\right), \tag{10}$$

$$\Re_k=\frac{\sin\left(2\pi f_k T_s L\right)}{\sin\left(2\pi f_k T_s\right)}, \tag{11}$$

$$\overset{\Delta}{\boldsymbol{E}}_r=\sum_{n=l}^{L+r-1}\left(\sum_{i=1}^{K}\sum_{\substack{j=1\\ j\neq i}}^{K}\left(y_i(n)y_j(n)\right)\right). \tag{12}$$

Thirdly, the total energy of $\boldsymbol{H}$ can be obtained by summing the energies of all the rows as:

$$\boldsymbol{E}=\sum_{r=1}^{L}\left(\bar{\boldsymbol{E}}_r\right)=\sum_{r=1}^{L}\overset{\Theta}{\boldsymbol{E}}_r+\sum_{r=1}^{L}\overset{\Delta}{\boldsymbol{E}}_r, \tag{13}$$

where

$$\sum_{r=1}^{L}\overset{\Theta}{\boldsymbol{E}}_r=\sum_{k=1}^{K}\left(\frac{A_k^2}{2}\left(L^2+\left(\Re_k\right)^2\cos\left(4\pi f_k T_s(L-1)+2\phi_k\right)\right)\right), \tag{14}$$

$$\sum_{r=1}^{L}\overset{\Delta}{\boldsymbol{E}}_r=\sum_{k=1}^{K}\left(\sum_{\substack{j=1\\ j\neq k}}^{K}\left(\sum_{r=1}^{L}\left(\sum_{n=r}^{L+r-1}\left(y_k(n)y_j(n)\right)\right)\right)\right). \tag{15}$$

Finally, the total energy $\boldsymbol{E}$ in (13) can be rewritten as:

$$\boldsymbol{E}=\boldsymbol{E}_1+\boldsymbol{E}_2+\ldots+\boldsymbol{E}_k+\ldots+\boldsymbol{E}_K=\sum_{k=1}^{K}\left(\widetilde{\boldsymbol{E}_k}+\Delta\boldsymbol{E}_k\right), \tag{16}$$

where

$$\widetilde{\boldsymbol{E}}_k=\left(\frac{A_k^2}{2}\left(L^2+\left(\Re_k\right)^2\cos\left(4\pi f_k T_s(L-1)+2\phi_k\right)\right)\right), \quad (17)$$

$$\Delta\boldsymbol{E}_k=\sum_{\substack{j=1\\ j\neq k}}^{K}\left(\sum_{r=1}^{L}\left(\sum_{n=l}^{L+r-1}\left(y_k(n)y_j(n)\right)\right)\right), \quad (18)$$

3) The relationship between $\widetilde{\boldsymbol{E}}_k$ and $\hat{\boldsymbol{E}}_k$

Aim of this paragraph is to investigate the relationship between $\widetilde{\boldsymbol{E}}_k$ and $\hat{\boldsymbol{E}}_k$. Equations (16)-(18) reveal that the energy of the k-th component $\boldsymbol{E}_k$ consists of two parts: $\widetilde{\boldsymbol{E}}_k$ in (17) represents the contribution of the k-th component itself, which depends on the length of data samples, sampling interval, and the k-th component's parameters (i.e., amplitude, frequency, phase). $\Delta\boldsymbol{E}_k$, instead, represents the influence of other components on the k-th component.

It is worth noting that $\overset{\Delta}{\boldsymbol{E}}_r$ in (12) represents the integral sum of the product of the components $y_i(t)$ and $y_j(t)$. If all $y_k(t)$ are harmonics and half-observation window (i.e., successive L samples of each row in $\boldsymbol{H}$) is coherent sampling, the product will be equal to zero due to the orthogonality of trigonometric functions. It also gives $\Delta\boldsymbol{E}_k$ in (18) equal to zero, as well as $\hat{\boldsymbol{E}}_k$ equal to $\widetilde{\boldsymbol{E}}_k$. This characteristic guarantees the applicability of $\hat{\boldsymbol{E}}_k$ in model order determination for harmonic signals. Although the $\hat{\boldsymbol{E}}_k$ is no longer equal to $\widetilde{\boldsymbol{E}}_k$ under the conditions of asynchronous sampling (i.e., frequency deviation) or interharmonics, it still ensure a strong positive correlation (more discussion in the next section). Therefore, $\hat{\boldsymbol{E}}_k$ is more suitable for order determination than raw SVs.

C. Robust and Adaptive Model Order Determination Method

In this subsection, we propose a robust and adaptive order determination method based on the relationship between $\widetilde{\boldsymbol{E}}_k$ and $\hat{\boldsymbol{E}}_k$. The steps are divided into two stages: first, a modified relative difference (RD) method is adopted to obtain a rough estimation of the model order of the power signal, i.e., $\bar{K}$. Second, determining the final estimation of model order, i.e., $\hat{K}$, by using $\bar{K}$ and the energies corresponding to 'noise' components.

1) Obtaining rough estimation of model order

The key to rough estimation is figuring out the potential boundary between the signal energies and the noise energies. To achieve this, a modified RD method is designed, and the main steps are as follows:

Step 1: construct energy vector $\overline{\boldsymbol{S}}$ by using each pair of consecutive SVs corresponding to each component as:

$$\overline{\boldsymbol{S}}=\left[\sqrt{\hat{\boldsymbol{E}}_1},\ldots,\sqrt{\hat{\boldsymbol{E}}_k},\ldots,\sqrt{\hat{\boldsymbol{E}}_G}\right]. \quad (19)$$

Step 2: calculate the RD values of elements in $\overline{\boldsymbol{S}}$ as:

$$RD(k)=\frac{\overline{\boldsymbol{S}}(k)-\overline{\boldsymbol{S}}(k+1)}{\overline{\boldsymbol{S}}(k)}, \quad \forall k=1,2,\cdots,G. \quad (20)$$

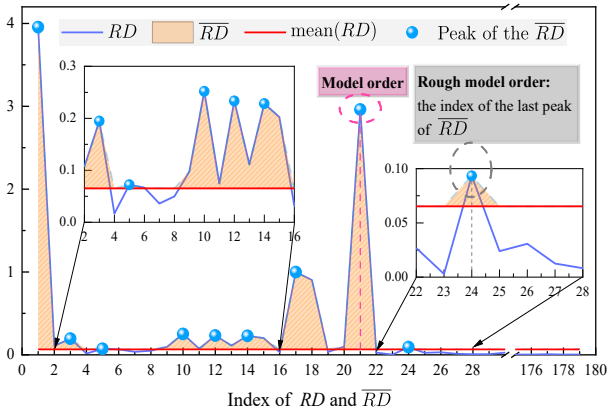

Fig. 1. Estimating the rough model order by the $\overline{RD}$ (*SNR*=35dB).

Step 3: obtain a rough estimation of model order, i.e., $\bar{K}$. First, calculating the mean value of *RD*. Second, construct $\overline{RD}$ by setting each *RD*(k) equal to the mean value if *RD*(k) lower than it. This is used to highlight the important energy differential nodes. In general, the boundary of signal and noise might be one of the largest values in $\overline{RD}$. Here, the index of the last peak of $\overline{RD}$ is regarded as the rough estimation of model order $\bar{K}$. It is worth noting that the number of peaks may be equal to zero under strong noise conditions. In this special situation, let $\bar{K}=1$.

After obtaining rough estimation of model order, the possible energies of the signal components can be regarded as $\overline{\boldsymbol{S}}(1)$, $\overline{\boldsymbol{S}}(2)$, $\cdots$, $\overline{\boldsymbol{S}}(\bar{K})$. The possible energies of the 'noise' components can be considered as $\overline{\boldsymbol{S}}(\bar{K}+1)$, $\overline{\boldsymbol{S}}(\bar{K}+2)$, $\cdots$, $\overline{\boldsymbol{S}}(G)$.

2) Final estimation of model order

In fact, the RD-based methods are only able to find the correct boundary in a situation with a high SNR. Here, a more robust method, which uses the possible energies of 'noise' components, is proposed to handle low SNR scenarios. The core idea is to establish a threshold ε using the mean value of the energies of the 'noise' components, and then determine the number of the signal components by comparing the elements of $\overline{\boldsymbol{S}}$ with ε. The main steps are as follows:

Step 1: calculate the threshold ε for separating signal components from the noise:

$$\varepsilon=\mathrm{V_{TH}}\cdot\frac{\overline{\boldsymbol{S}}(\bar{K}+1)+\overline{\boldsymbol{S}}(\bar{K}+2)+\cdots+\overline{\boldsymbol{S}}(G)}{G-\bar{K}}, \quad (21)$$

where $\mathrm{V_{TH}}$ represents the threshold sensitivity coefficient which is determined by the statistical analysis of experimental results (in this paper, $\mathrm{V_{TH}}$ is set to 5). It is worth noting that $\mathrm{V_{TH}}$ does not need to be changed according to SNR, window length, and sampling rate during the whole estimation process.

Step 2: determine the model order of the signal. If $\overline{\boldsymbol{S}}(k)>\varepsilon$, $\overline{\boldsymbol{S}}(k)$ can be treated as one element of the signal. Finally,

let $\widehat{K}$ be equal to the number of elements in $\overline{\boldsymbol{S}}(k)$ greater than the threshold ε. Such $\widehat{K}$ is then the model order of the analyzed power signal.

III. Results and Discussion

In this section, simulations are conducted to evaluate the effectiveness and robustness of the proposed method. From Equations (16)-(18), it is clear that the larger the number of signal components, the harder it is to estimate the correct number of signal components. The classical synthetic signal suggested in [16] contains twelve components. To prove the robustness of the proposed method, the test signals should have two features: 1) the number of signal components should be larger than the classical synthetic signal; 2) the parameters of the signal components should be random values within a reasonable range based on [21]. Thus, each test signal contains a fundamental and twenty other components (either harmonics or interharmonics). The nominal frequency of the test signal is f_n = 50 Hz while the amplitude of twenty other components is a random value in the range of [1 %, 20 %) of the fundamental. The phase of all components is a random value in the range of [-π, π). Three types of test signals are considered: ***a***) synchronously sampled (f_1 = 50 Hz) signals containing a fundamental and twenty harmonics; ***b***) asynchronously sampled (f_1 = 50 Hz ± 2 or 5 Hz) signals containing the fundamental and twenty harmonics; ***c***) signals containing a fundamental and twenty interharmonics (the interval between any two frequencies meets the definitions of interharmonics in the IEC Std 61000-4-7 [21]).

A. $\widehat{\boldsymbol{E}}_k$ and $\widetilde{\boldsymbol{E}}_k$ Under Different Conditions

To demonstrate that $\widehat{\boldsymbol{E}}_k$ is suitable for the model order determination under different conditions, the relationship of

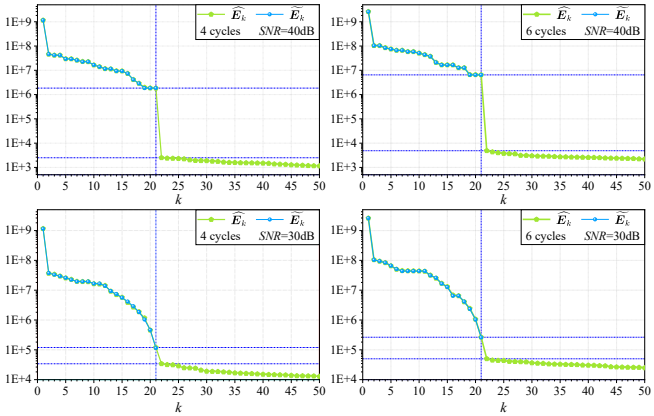

Fig. 2. $\widehat{\boldsymbol{E}}_k$ and $\widetilde{\boldsymbol{E}}_k$ under the harmonics conditions (coherent sampling).

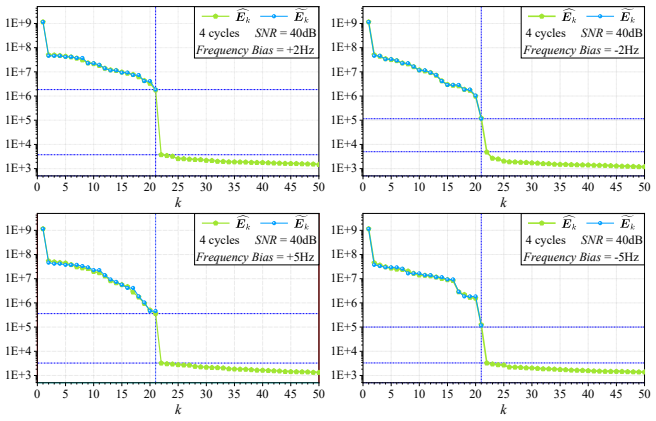

Fig. 3. $\widehat{\boldsymbol{E}}_k$ and $\widetilde{\boldsymbol{E}}_k$ under the harmonics conditions (asynchronous sampling).

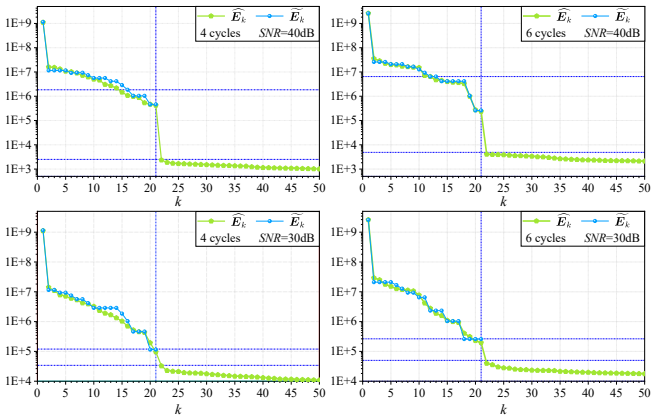

Fig. 4. $\widehat{\boldsymbol{E}}_k$ and $\widetilde{\boldsymbol{E}}_k$ under the interharmonics conditions.

$\widehat{\boldsymbol{E}}_k$ and $\widetilde{\boldsymbol{E}}_k$ is investigated by simulations. A sampling rate of f_s = 12 kHz, and two different observation window lengths, 4 or 6 cycles (N = 959 or 1439), are considered. All test signals are superposed with 30 dB or 40 dB noise.

The test results under the coherent and asynchronous sampling conditions are reported in Fig. 2 and Fig. 3, respectively. It can be observed that the curves representing $\widehat{\boldsymbol{E}}_k$ and $\widetilde{\boldsymbol{E}}_k$ are almost overlapped in the presence of all considered observation window lengths and noise levels conditions. The test results under the twenty interharmonics conditions are reported in Fig. 4. Although the curves representing $\widehat{\boldsymbol{E}}_k$ and $\widetilde{\boldsymbol{E}}_k$ do not completely overlap, they maintain a strong correlation trend. Moreover, there is a distinct gap between $\widehat{\boldsymbol{E}}_{21}$ (the smallest one contributed by interharmonics) and $\widehat{\boldsymbol{E}}_{22}$ (the largest one contributed by noise). Therefore, $\widehat{\boldsymbol{E}}_k$ is a reasonable indicator for order determination.

B. Success Rate of the Proposed Method in Order Estimation

The Monte Carlo simulations are conducted to evaluate the behaviour of the proposed method while estimating the model order. The performance is also compared with the MEMO method. Two different sampling rates (f_s = 6 and 12 kHz) and two different observation window lengths (C = 4 and 6 cycles) are considered. Gaussian white noise is superimposed on three

types of representative test signals to evaluate success rates under different SNRs, which range from 20 to 50 dB at an increment of 1 dB. For each test, 1000 runs are performed to evaluate the statistical properties.

The results are presented in Fig. 5. It can be observed that the success rates are positively correlated with the number of samples for all test conditions (harmonics or interharmonics). The proposed method offers better robustness compared with the MEMO method within all considered data sample lengths. Moreover, even if the proposed method uses the fewest data samples (i.e., f_s = 6kHz, C = 4, N = 479), the behaviour is still better than that of MEMO which uses the maximum data samples (i.e., f_s = 12kHz, C = 6, N = 1439). In consideration of the SVD is a time-consuming technique, it means that the proposed method only requires a smaller computational burden to achieve the same performance.

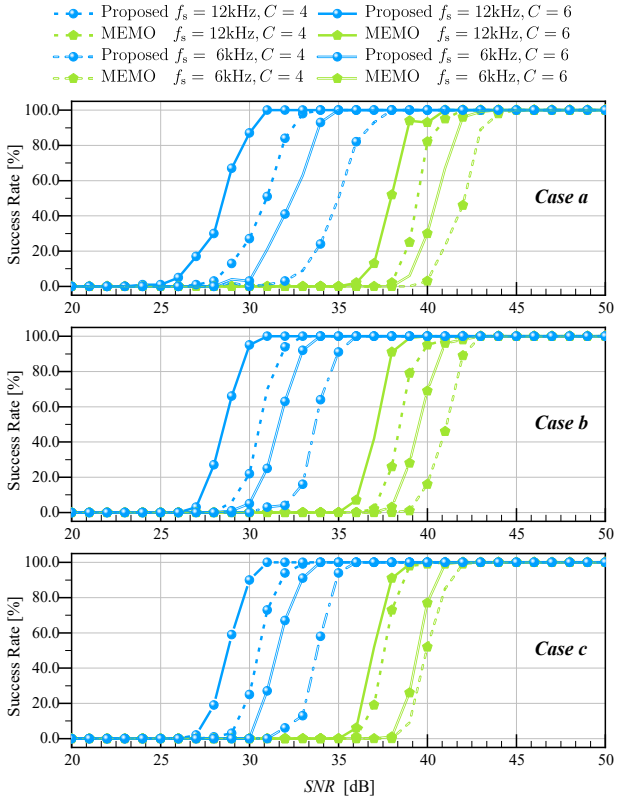

Fig. 5. Success rate of methods under different conditions. ***Case a*****:** f_1 = 50Hz, twenty harmonics, coherent sampling; ***Case b*****:** f_1 = 50Hz±5Hz, twenty harmonics, asynchronous sampling; ***Case c*****:** f_1 = 50Hz, twenty interharmonics.

IV. CONCLUSIONS

In this paper, a novel model order determination method is presented for signals containing harmonics and inter-harmonics. The contribution is twofold: firstly, a novel and efficient indicator is proposed based on the relationship between each component and raw SVs. Secondly, a robust and adaptive order determination procedure is proposed to obtain the model order independently of the noise levels. Simulation results show that the behaviour of the proposed method outperforms the MEMO method. This is particularly true when the SVs of the noise and components have only small relative differences (e.g., signals defined in Section III under SNR < 40dB conditions) even if fewer data samples are used. It can be concluded that is implementable into SVD-based methods to improve its performance. In particular, for distinguishing weak harmonics or interharmonics from the measurement environment with unknown noise levels.

ACKNOWLEDGEMENT

This work was supported in part by the National Natural Science Foundation of China under Grant 61771190, and in part by science and technology innovation Program of Hunan Province under Grant 2021RC4020, and in part by the China Scholarship Council under Grant 202006130143.

REFERENCES

[1] H. Wen, J. H. Zhang, Z. Meng, S. Y. Guo, F. H. Li, and Y. X. Yang, "Harmonic Estimation Using Symmetrical Interpolation FFT Based on Triangular Self-Convolution Window," *Ieee Transactions on Industrial Informatics,* vol. 11, no. 1, pp. 16-26, Feb, 2015.

[2] X. Lin, J. Yu, R. Yu, J. Zhang, Z. Yan, and H. Wen, "Improving Small-Signal Stability of Grid-Connected Inverter Under Weak Grid by Decoupling Phase-Lock Loop and Grid Impedance," *IEEE Transactions on Industrial Electronics,* vol. 69, no. 7, pp. 7040-7053, 2022.

[3] Z. Yan, and H. Wen, "Electricity Theft Detection Base on Extreme Gradient Boosting in AMI," *IEEE Transactions on Instrumentation and Measurement,* vol. 70, pp. 1-9, 2021.

[4] J. Song, J. Zhang, H. Kuang, and H. Wen, "Dynamic Synchrophasor Estimation Based on Weighted Real-Valued Sinc Interpolation Method," *IEEE Sensors Journal,* vol. 23, no. 1, pp. 588-598, 2023.

[5] S. K. Jain, P. Jain, and S. N. Singh, "A Fast Harmonic Phasor Measurement Method for Smart Grid Applications," *IEEE Transactions on Smart Grid,* vol. 8, no. 1, pp. 493-502, 2017.

[6] J. Song, A. Mingotti, J. Zhang, L. Peretto, and H. Wen, "Fast Iterative-Interpolated DFT Phasor Estimator Considering Out-of-Band Interference," *IEEE Transactions on Instrumentation and Measurement,* vol. 71, pp. 1-14, 2022.

[7] T. Jin, and W. Zhang, "A Novel Interpolated DFT Synchrophasor Estimation Algorithm With an Optimized Combined Cosine Self-Convolution Window," *IEEE Transactions on Instrumentation and Measurement,* vol. 70, pp. 1-10, 2021.

[8] J. Li, H. Liu, T. Bi, and J. Zhao, "Second-order matrix pencil-based phasor measurement algorithm for P-class PMUs," *IET Generation, Transmission & Distribution,* vol. 14, no. 19, pp. 3953-3961, 2020.

[9] P. W. Pande, B. R. Kumar, S. Chakrabarti, S. C. Srivastava, S. Sarkar, and T. Sharma, "Model order estimation methods for low frequency oscillations in power systems," *International Journal of Electrical Power & Energy Systems,* vol. 115, 2020.

[10] J. Song, A. Mingotti, J. Zhang, L. Peretto, and H. Wen, "Accurate Damping Factor and Frequency Estimation for Damped Real-Valued Sinusoidal Signals," *IEEE Transactions on Instrumentation and Measurement,* vol. 71, pp. 1-4, 2022.

[11] P. Banerjee, and S. C. Srivastava, "An Effective Dynamic Current Phasor Estimator for Synchrophasor Measurements," *IEEE Transactions on Instrumentation and Measurement,* vol. 64, no. 3, pp. 625-637, Mar, 2015.

[12] G. W. Chang, and C.-I. Chen, "An Accurate Time-Domain Procedure for Harmonics and Interharmonics Detection," *IEEE Transactions on Power Delivery,* vol. 25, no. 3, pp. 1787-1795, 2010.

[13] L. Bernard, S. Goondram, B. Bahrani, A. Pantelous, and R. Razzaghi, "Harmonic and Interharmonic Phasor Estimation using Matrix Pencil Method for Phasor Measurement Units," *IEEE Sensors Journal*, pp. 1-1, 2020.

[14] J. Song, J. Zhang, and H. Wen, "Accurate Dynamic Phasor Estimation by Matrix Pencil and Taylor Weighted Least Squares Method," *IEEE Transactions on Instrumentation and Measurement,* vol. 70, pp. 1-11, 2021.

[15] J. Chen, X. Li, M. A. Mohamed, and T. Jin, "An Adaptive Matrix Pencil Algorithm Based-Wavelet Soft-Threshold Denoising for Analysis of Low Frequency Oscillation in Power Systems," *IEEE Access,* vol. 8, pp. 7244-7255, 2020.

[16] S. K. Jain, and S. N. Singh, "Exact Model Order ESPRIT Technique for Harmonics and Interharmonics Estimation," *IEEE Transactions on Instrumentation and Measurement,* vol. 61, no. 7, pp. 1915-1923, 2012.

[17] J. Chen, T. Jin, M. A. Mohamed, and M. Q. Wang, “An Adaptive TLS-ESPRIT Algorithm Based on an S-G Filter for Analysis of Low Frequency Oscillation in Wide Area Measurement Systems,” *Ieee Access,* vol. 7, pp. 47644-47654, 2019.

[18] Z. D. Drummond, K. E. Claytor, D. R. Allee, and D. M. Hull, “An Optimized Subspace-Based Approach to Synchrophasor Estimation,” *IEEE Transactions on Instrumentation and Measurement,* vol. 70, 2021.

[19] S. K. Jain, S. N. Singh, and J. G. Singh, “An Adaptive Time-Efficient Technique for Harmonic Estimation of Nonstationary Signals,” *IEEE Transactions on Industrial Electronics,* vol. 60, no. 8, pp. 3295-3303, Aug, 2013.

[20] K. Konstantinides, and K. Yao, “Statistical analysis of effective singular values in matrix rank determination,” *IEEE Transactions on Acoustics, Speech, and Signal Processing,* vol. 36, no. 5, pp. 757-763, 1988.

[21] I. S. 61000‐4‐7, “Electromagnetic compatibility (EMC)‐part 4‐7: testing and measurement techniques‐general guide on harmonics and interharmonics measurements and instrumentation, for power supply systems and equipment connected thereto,” 2009.